Chinese Chemical Letters 34 (2023) 108104

Contents lists available at ScienceDirect

Chinese Chemical Letters

journal homepage: www.elsevier.com/locate/cclet

Local sustained release of PD-1 monoclonal antibody and lenvatinib by thermo-sensitive hydrogel for improving tumor immunotherapy

Lin Zhai[a,1], Yujie Shi[a,b,1], Yi Yan[a], An Lu[a], Xiaoyu Liu[a], Lei Lei[a], Yi Sun[a], Linxia Jiang[a], Xiangyu Wang[a], Honggang Qian[c,*], Jiancheng Wang[a,*]

[a] Beijing Key Laboratory of Molecular Pharmaceutics and New Drug Delivery Systems, State Key Laboratory of Natural and Biomimetic Drugs, School of Pharmaceutical Sciences, Peking University, Beijing 100191, China
[b] Department of Pharmaceutical Analysis, School of Pharmaceutical Sciences, Peking University, Beijing 100191, China
[c] Key Laboratory of Carcinogenesis and Translational Research (Ministry of Education), Department of Hepato-Pancreato-Biliary Surgery, Peking University Cancer Hospital & Institute, Beijing 100142, China

ARTICLE INFO

Article history:
Received 12 September 2022
Revised 22 December 2022
Accepted 25 December 2022
Available online 20 March 2023

Keywords:
Lenvatinib
PD-1 antibody
Thermosensitive hydrogels
Topical administration
Tumor immunotherapy

ABSTRACT

In clinic, the combination of intravenous pembrolizumab (PD-1 monoclonal antibody) with oral Lenvatinib (LEN) exhibited an enhanced synergistic benefit for cancer therapy. However, the clinical outcomes were always limited by the problems of inconsistent pharmacokinetic profiles of two drugs, lower drug accumulation in tumor and obvious side effects during the combination therapy. Here, *in situ*-forming thermosensitive hydrogels based on PLGA-PEG-PLGA triblock copolymers were prepared for local administration of anti-PD1 and LEN (P&L@Gel) to improve therapeutic efficacy and safety. After peritumoral or surgical resection site injection, the significant increased concentrations of both drugs in tumor were observed with the local sustained release of P&L@Gel. In comparison with the group of intraperitoneal anti-PD1 plus oral LEN (P-ip&L-po), significantly higher tumor inhibition efficiency on CT26 tumor models could be obtained in P&L@Gel group, even at the dose of one-eighth of the former, same tumor-inhibition effects could be achieved. The enhanced antitumor efficacy of P&L@Gel group was probably associated with the 2.2 folds of increased level of CD8+ T cells and the polarization of tumor associated macrophage from M2 to M1 along with the increased drug accumulation. Moreover, compared with the obvious side effects of P-ip&L-po group, no significant changes of PLT, ALT and UA in blood, as well as IL-1α and IL-1β in mice paws were observed between P&L@Gel group and untreated group. These results suggested that local administration of anti-PD1 and LEN with thermosensitive hydrogel could offer a potential strategy for tumors or tumor postoperative adjuvant treatment.

Due to the low overall response rates (<20%) and the complexity and heterogeneity of tumor microenvironment (TME), PD-1 blockade based immunotherapies are difficult to achieve in solid tumor patients [1–4]. Moreover, within TME, abnormal tumor neovascularization can foster protumoral immune cell evasion, disturb anti-cancer immunity and promote tumor growth [5]. Therefore, the combination therapy of immune checkpoint inhibitors (ICIs) and tumor vascular targeted drugs may be a potential solution to improve anti-tumor immunity and overcome the low response rates to ICIs [5–7]. In clinic, the combination of intravenous pembrolizumab (PD-1 monoclonal antibody) with oral Lenvatinib (LEN) exhibited a synergistic effect and improved benefit for cancer therapy.

LEN, a tyrosine kinase inhibitor, can selectively block vascular endothelial growth factor receptor (VEGFR) 1-3 and fibroblast growth factor receptor (FGFR)1-4 [8,9]. In a phase Ib clinical trail (NCT03006926) [10], the combination of lenvatinib and pembrolizumab (anti-PD1) showed a significant improvement clinical benefit for patients with advanced hepatocellular carcinoma (HCC). The clinical trail results showed that patients treated with lenvatinib combined with anti-PD1 had objective response rate (ORR) of 46.0% per mRECIST and 36.0% per RECIST v1.1, and median progression-free survival of 9.3 months and 8.6 months, respectively. Because of the remarkable efficacy, this combination strategy was approved by FDA as a breakthrough therapy for the first-line treatment of HCC [11–13]. The likely combination mechanism was related with the simultaneous blocking of VEGFR and

* Corresponding authors.
E-mail addresses: qianhg@sohu.com (H. Qian), wang-jc@bjmu.edu.cn (J. Wang).
[1] These authors contributed equally to this work.

https://doi.org/10.1016/j.cclet.2022.108104
1001-8417/

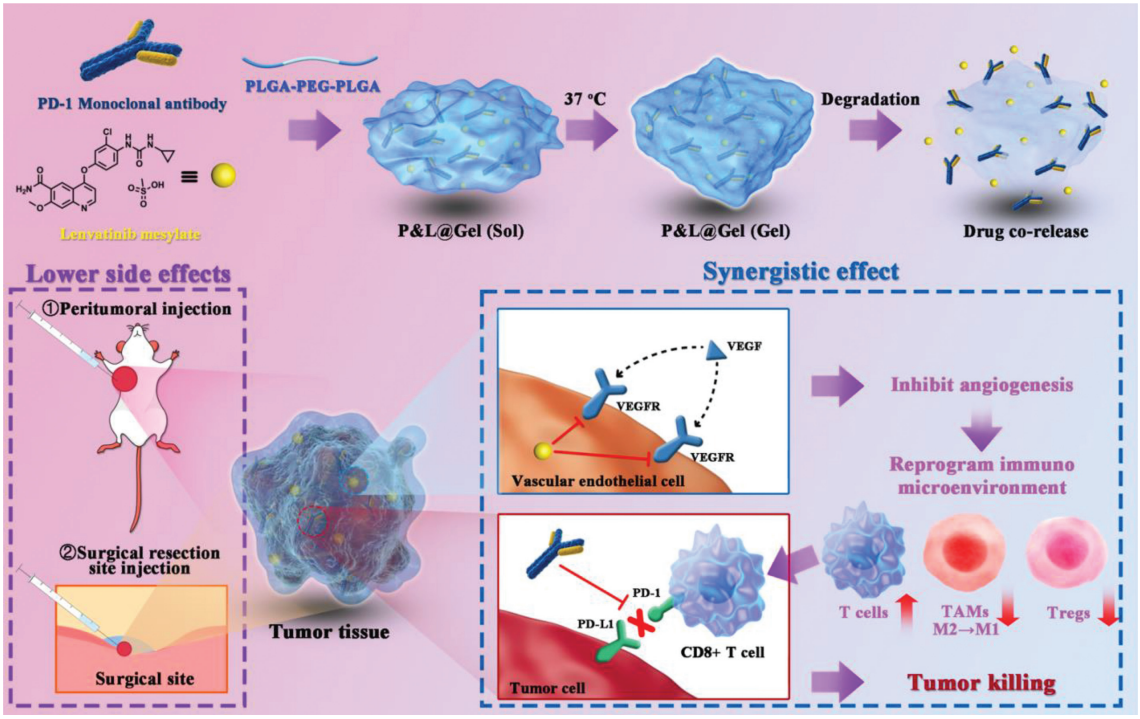

Scheme 1. The schematic illustration of P&L@Gel as a novel thermosensitive agent for synergistic anticancer therapy.

PD-1 [14,15]. However, obvious side effects were observed clinically because both drugs were administered systemically in the actual combination strategy, *i.e.*, oral lenvatinib once daily and intravenous PD-1 monoclonal antibody once every three weeks. The most common treatment-related adverse events (AEs) in the combination of pembrolizumab and lenvatinib were hypertension, fatigue, palmar-plantar erythrodysesthesia syndrome (PPES), elevated aminotransferase (ALT or AST) levels, *etc.* [16]. The rate of AEs ($\geq$ grade 3) in solid cancer was ~70%, and more than 50% of patients require drug dose reduction or even discontinuance during clinical trials due to treatment-related adverse events [16]. In addition, different physicochemical properties, *in vivo* pharmacokinetics, tissue distribution and cell penetration behavior between LEN and PD-1 antibody limited the synergistic therapeutic effects. Therefore, to develop a local co-delivery strategy is important for improving efficacy and reducing toxicity of the combination of LEN and anti-PD1.

Here, poly(lactic acid-*co*-glycolic acid)-*b*-poly(ethylene glycol)-*b*-poly(lactic acid-*co*-glycolic acid) (PLGA-PEG-PLGA), a biodegradable triblock copolymer named ReGel® [17,18], was used to fabricate a temperature-sensitive *in-situ* gel for local administration of anti-PD1 and lenvatinib mesylate (P&L@Gel), to treat tumors or serve as tumor postoperative adjuvant therapy (Scheme 1). We propose that local combination of checkpoint blocking immunotherapy and anti-angiogenesis therapy may be meaningful for oncotherapy.

To obtain sustained drug release after peritumoral or surgical resection site injection, PLGA-PEG-PLGA triblock copolymer hydrogel was selected as a depot. Firstly, the *in vitro* safety of the copolymer material was proved by its no influence on cell viability assayed with MTT after 72 h incubation on 3T3 cell line (Fig. S1A in Supporting information) and CT26 cell line (Fig. S1B in Supporting information). The LEN-loaded hydrogel (L@Gel) prepared by dissolving LEN into PLGA-PEG-PLGA hydrogel (20 wt%) was further mixed with anti-PD1 solution to form the final P&L@Gel preparation (Fig. S2 in Supporting information). The phase diagram of PLGA-PEG-PLGA copolymer aqueous solution (20 wt%) was determined by test-tube-inversion method and the results were shown in Fig. S1C (Supporting information). At 4 °C, P&L@Gel appeared as fluid and flowed freely with gravity. When the temperature increased to 37 °C, the 20 wt% hydrogel was physically transformed from sol to gel (Fig. 1A). Besides, the thermosensitive transitions of both blank hydrogel and P&l@Gel were investigated by rheological measurements. As shown in Fig. S3 (Supporting information), the storage modulus (*G'*) and loss modulus (*G"*) of the two hydrogels measured were low at initial temperature, indicating the well flowability and injectability of samples. As temperature increased around body temperature, G' and G" raised corresponding with the process of gelation. When G' and G" met each other, the temperature was noted as the gelation temperature [19]. The gelation temperature found in the rheological analysis were 32 °C and 37 °C for blank hydrogel and P&L@Gel, respectively. The difference of the gelation temperature between the two preparations was caused by the loaded drugs in P&L@Gel. As reported, PLGA-PEG-PLGA triblock copolymers tended to self-assemble into micelles at lower temperatures. The hydrophobic interactions of PLGA blocks were enhanced and the PEG shell was dehydrated with the temperature increased. Then, the micelles accumulated and inter-micellar aggregation formed to realize the sol-to-gel phase transition. The gelation temperature was attributed to the ratio of hydrophobic and hydrophilic components of the preparations as well as the weight percent concentration of the copolymer solution [20,21]. After loading drugs, hydrophobic LEN and hydrophilic anti-PD1 into the hydrogel, the ratio of hydrophobic and hydrophilic components was changed. Thus, the gelation temperature of P&L@Gel showed unequal to blank hydrogel. To sum up, the gelation temperature of both P&L@Gel and blank hydrogel showed lower than body temperature, which could meet the demand of gelation *in situ*.

Next, the stability of P&L@Gel was evaluated by determining the concentrations of LEN and anti-PD1 containing in the top, middle and bottom of hydrogel after the storage for 30 days at 4 °C using high performance liquid chromatography (HPLC) and enzyme-linked immunosorbent assay (ELISA) kit, respectively. There was no

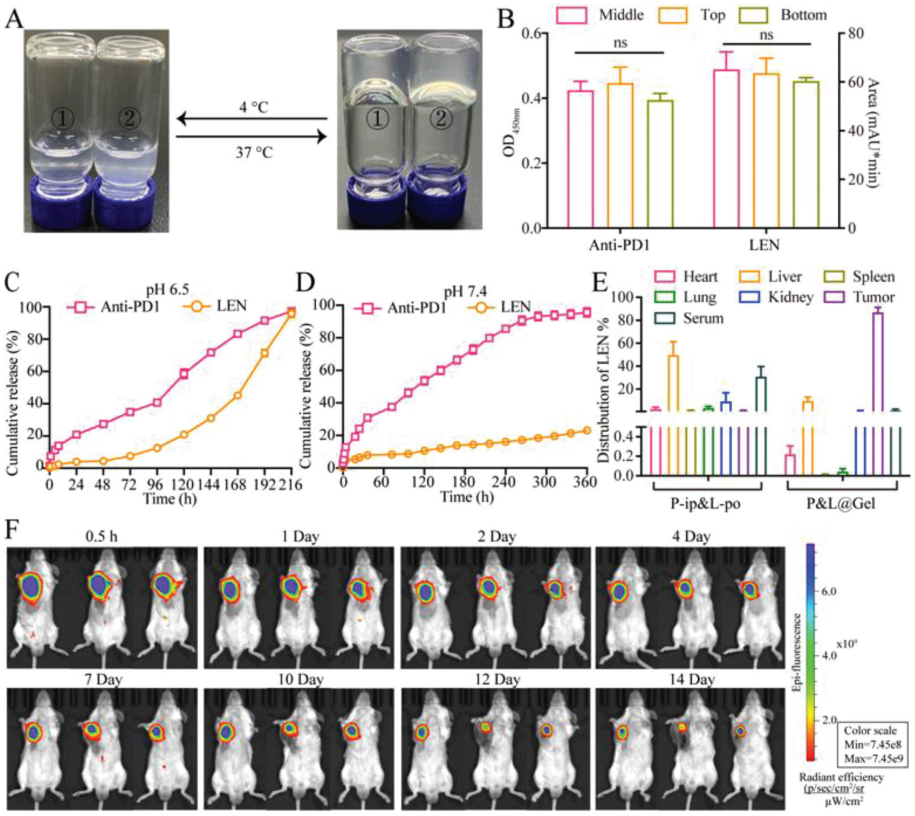

Fig. 1. (A) Reversible sol-to-gel phase transition of hydrogels between 4 °C and 37 °C (① blank hydrogel, ② P&L@Gel). (B) The concentration of drugs in the top, middle and bottle part of P&L@Gel after 30 days storage ($n = 3$). *In vitro* drug release at pH 6.5 (C) and pH 7.4 (D) of P&L@Gel ($n = 3$). (E) The biodistribution of LEN in mice treated with P-ip&L-po and P&L@Gel on the 5th day ($n = 5$). (F) The biodistribution of Cy5-IgG in mice treated with drug loaded hydrogel. Data represent mean ± S.D.

significant difference in the concentrations of LEN and anti-PD1 in the top, middle and bottom parts of P&L@Gel (Fig. 1B). Besides, no obvious drug precipitate or aggregation could be observed on the 30th day. And either the blank hydrogel or P&L@Gel could realize sol-to-gel transition after the storage (Figs. S4A and B in Supporting information). These results further indicated the high stability of the P&L@Gel formulation.

The proportion of PLGA-PEG-PLGA copolymers was optimized by the gelation temperature according to the state of sol-to-gel. As shown in Fig. S1C, the gelation temperature was decreased as the weight percent (wt%) of the PLGA-PEG-PLGA copolymers increased. At physiological temperature (~37 °C), the optimum weight percent of the copolymer that exhibited a sol-to-gel transition was 20 wt% to 25 wt%. Considering that the 25 wt% gel was slightly viscous than 20 wt%, 20 wt% gel was chosen as drug vehicle for subsequent experiments.

The morphology of the 20 wt% hydrogels with or without drugs were observed by Cryo-scanning electron microscope (Cryo-SEM) (Figs. S4C and D in Supporting information). It was demonstrated that there was no significant difference in porous structure between blank hydrogel and P&L@Gel, and no obvious drug precipitation observed in P&L@Gel.

In order to estimate the pharmacokinetic profiles of two drugs, drug release *in vitro* and distribution *in vivo* were studied. The cumulative release profiles of anti-PD1 and LEN in PBS at pH 6.5 could be maintained for 216 h (9 days) (Fig. 1C). As shown in Fig. 1D, the release time of drug-loaded hydrogel could sustain for more than 2 weeks in PBS at pH 7.4. The different drugs release behaviors in two environments were owing to the different physical and chemical properties of the two drugs and the degradation behavior of the hydrogel. For anti-PD1, there was no significant different release profile between PBS at pH 6.5 and pH 7.4. As a hydrophilic drug, anti-PD1 was released mainly through diffusion from P&L@Gel. While the release behavior of LEN differed at these two conditions, which was owing to the different solubility of LEN and degradation behaviors of the hydrogel. Hydrophobic drug LEN showed gradual release mainly by hydrogel degradation accelerated by the acid environment (pH 6.5), rather than by diffusion [22–24]. In tumor microenvironment (pH 6.5), anti-PD1 and LEN could be released almost simultaneously in PBS on account of the boosted release of LEN with the degradation of hydrogel, which was more favourable for anti-tumor efficacy.

Moreover, the biodistribution of LEN was investigated by LC-MS/MS. As shown in Fig. 1E, ~87% of LEN (including the total amount of serum, tumor, heart, liver, spleen, lung and kidney) were accumulated at the tumor site after treated with P&L@Gel, which was significantly higher than that of P-ip&L-po (less than 2%). The higher accumulation of LEN after treated with P&L@Gel was benefit for the therapeutic effects.

To evaluate the biodistribution of anti-PD1, Cy5-IgG, served as an alternative of anti-PD1 [25], was loaded into 20 wt% PLGA-PEG-PLGA hydrogel. After peritumoral injected on CT26 tumor bearing mice, the fluorescence of Cy5 was monitored by real-time fluorescence imaging. The fluorescence of Cy5 in mice (Fig. 1F) showed the high accumulation in tumor sites for more than 2 weeks. On the 14th day, the mice were sacrificed due to the large tumor volumes. Besides, as presented in supplementary data (Fig. S5 in Supporting information), Cy5-IgG could retain at normal microenvironment for about one month when subcutaneously injected to health mice. In the control groups of both tumor-bearing mice (Figs. S6A and C in Supporting information) and normal mice (Figs. S6B and D in Supporting information), the fluorescence of Cy5-IgG in normal saline could only maintain at the injected site for 36-48 h. On one hand, these results demonstrated that most of

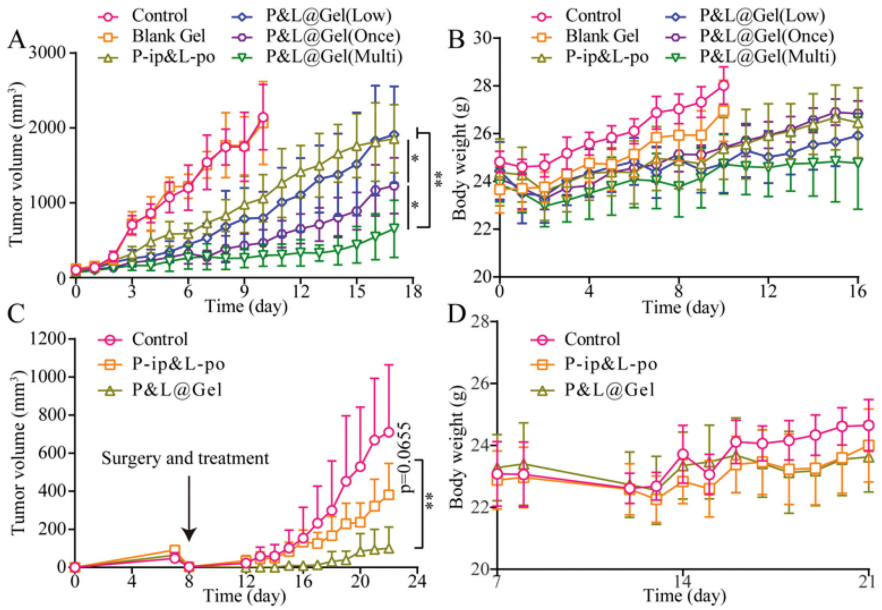

Fig. 2. (A, B) *In vivo* antitumor effects of P&L@Gel ($n = 5$). (A) The tumor growth curve of CT26 tumor-bearing BALB/c mice model during the treatment. (B) The body weight of mice during the treatment. (C, D) *In vivo* inhibition effects of P&L@Gel on tumor recurrence after surgery ($n = 6$). (C) The tumor growth curve of mice during the treatment. (D) The body weight of mice during the treatment. Data represent mean ± S.D. $^{*}P < 0.05$, $^{**}P < 0.01$, $^{***}P < 0.001$.

anti-PD1 were distributed in the target site by hydrogel. On the other hand, it could be indicated that P&L@Gel was able to realize long retention *in vivo*. The favourable distribution and local retention behavior of P&L@Gel were the key to its better efficacy.

To validate whether localized administration of P&L@Gel could enhance the combination therapeutic effects of two drugs, the tumor inhibition of P&L@Gel was evaluated on CT26 tumor model. Balb/c mice bearing CT26 tumors were obtained and they were grouped and received various treatments (Fig. S7A in Supporting information). All animal experiments were approved by the Animal Ethics Committee of Peking University. Since the *in-situ* hydrogel could achieve sustained drug release and prolong retention in administration site, single dose of P&L@Gel(Once) was given to investigate the long-term tumor inhibition effect. Considering the dose-dependent therapeutic effects on CT26 tumor, P&L@Gel(Multi) was used to optimize treatment regimen, and P&L@Gel(Low) was designed to explore whether the dose could be further reduced and ensure the efficacy at the same time on account of the probably enhanced synergistic effect after local administration. As shown in Fig. 2A, tumor volume of mice in saline group and blank gel group increased sharply compared with those of other groups, indicating that blank hydrogel had no effect on tumor inhibition. Compared with P-ip&L-po, P&L@Gel(Low), P&L@Gel(Once) and P&L@Gel(Multi) showed similar (1910.61 mm^3 *vs.* 1855.18 mm^3), 33.78% smaller (1228.58 mm^3 *vs.* 1855.18 mm^3) and 64.79% smaller (653.24 mm^3 *vs.* 1855.18 mm^3) tumor volumes, respectively. During the whole treatment, the total dose of P-ip&L-po was approximately 8 folds, 6 folds and 2 folds of that of P&L@Gel(Low), P&L@Gel(Once) and P&L@Gel(Multi), respectively. No obvious weight loss was observed among these groups (Fig. 2B). The tumor growth inhibition rate of P&L@Gel(Multi) reached approximately 86% on the 10^{th} day. Since the average tumor volume reached 2000 mm^3 on the 10^{th} day, the mice of control group and blank gel group were sacrificed according to laboratory animal welfare and ethics. The tumor volume and body weight of mice in other groups were calculated until the end of the experiment on the 17^{th} Day. These results indicated that peritumoral administration of P&L@Gel could remarkably improve the anti-tumor efficacy, and same or better therapeutic effects could be obtained in lower dosage.

Despite surgical technology improvement, tumor recurrence still occurs usually for the exist of residual tumor micro-infiltration and circulating tumor cells after resection. Potential strategy for tumor postoperative adjuvant treatment was explored extensively. Therefore, incompletely resected CT26-tumor models were established successfully in this study to verify the tumor recurrence inhibition efficacy of P&L@Gel (Fig. S7B in Supporting information). The growth of tumor residues and body weight were monitored daily from the 4^{th} postoperative day until the end of the experiment (Figs. 2C and D). As expected, the mice in P&L@Gel group showed the slowest rate of tumor regrowth with three of six mice experiencing no tumor recurrence until the end of the treatment (Figs. S7D and E in Supporting information). Besides, the body weights of mice in all groups were not impacted by the treatment (Fig. 2D). The tumor weight on the 22^{nd} Day (Fig. S7C in Supporting information) of the P&L@Gel group was also the lowest among all the treatment groups, which was corresponding with the tumor volumes above. In this model, topical injection of P&L@Gel was more effective in suppressing tumor regrowth compared with P-ip&L-po, and the dose of the former was only ~1/5 that of the latter. Owing to the large individual variables, no significant difference was detected between control group and P-ip&L-po group in terms of tumor growth curve and *ex vivo* tumor weight. These results suggested that topical administration of P&L@Gel could obviously improve the inhibition of postoperative tumor recurrence.

It has been reported that LEN could inhibit angiogenesis and normalize tumor vessels by blocking VEGF/VEGFR pathway [26,27]. In this study, to verify the effect of LEN, the immunofluorescence staining of CD31 on vascular endothelium was examined on the 17^{th} day after various treatments. As shown in Fig. 3A, red fluorescence intensity of labeled CD31 in all LEN treated groups was weaker than control group and blank gel group, verifying the significant inhibition effect of LEN on abnormal tumor angiogenesis. Besides, the immune checkpoint inhibitor functioned by not only blocking PD-1 expressing on increased T cells, but also inducing the normalization of tumor vessels by CD4+ T cells and CD8+ T cells through IFN-γ pathway [5,14,28].

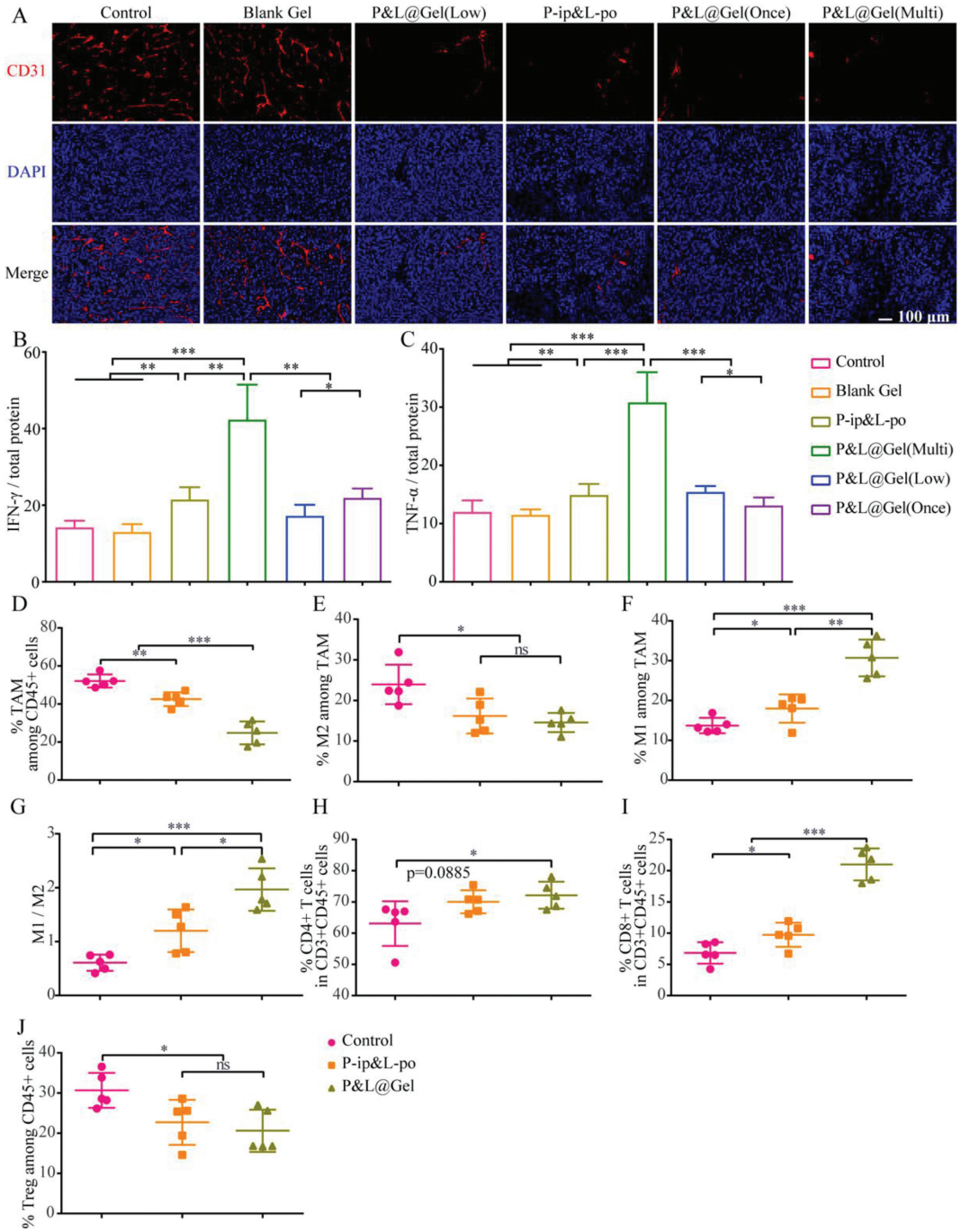

Fig. 3. P&L@Gel significantly improved the anti-tumor immune responses. (A) Immunofluorescence staining for tumor blood vessels in tumor tissues of each group on the 17th day. The CD31 on the vascular endothelial cells was stained red, and the cell nucleus was stained blue with DAPI. The level of IFN-γ (B) and TNF-α (C) in tumor tissues. (D-F, H-J) Relative quantification of TAMs, M2 macrophages, M1 macrophages, tumor-infiltrating T cells and Tregs in tumor tissues. (G) The ratio of M1/M2 in different groups. Date was presented as mean ± S.D. ($n = 5$). $^{*}P < 0.05$, $^{**}P < 0.01$, $^{***}P < 0.001$.

To further elucidate the underlying mechanisms of tumor inhibition of different groups, the antitumor-related cytokines and intratumoral profiles of immune cells were measured at the end of the therapy. Firstly, interferon-gamma (IFN-γ) and tumor necrosis factor-α (TNF-α) were detected by ELISA. As shown in Figs. 3B and C, P&L@Gel(Multi) group showed the highest levels of IFN-γ and TNF-α among all the groups. Besides, levels of these two cytokines in P&L@Gel(Multi) group was significantly higher (~2 folds) than that of the P-ip&L-po group (the total dose was only half of the latter), and the levels in the P&L@Gel(Once) group and P&L@Gel(Low) group were respectively similar to that of the P-ip&L-po group (the total dose was one-sixth and one-eighth of the latter, respectively). IFN-γ and TNF-α were originally found to be produced by inflammatory cells and played key roles in the immune system, surveillance of tumor growth and suppress sprouting angiogenesis [29]. In this study, the highest level of TNF-α in P&L@Gel(Multi) group corresponded to the result of fewer vessels observed (Fig. 3A) and strongest tumor inhibition effects (Fig. 2A) indicated that topical administration of P&L@Gel could remarkably activate the anti-tumor immunity response and exert a better synergistic effect.

Furthermore, flow cytometric assay was applied to investigate the intratumoral profiles of immune cells, including TAMs, T cells and regulatory cells (Tregs). Notably, after treatment with P-ip&L-

po and P&L@Gel, the population of TAM (Control *vs.* P-ip&L-po *vs.* P&L@Gel: 52.10 % *vs.* 42.55 % *vs.* 24.82 %) (Fig. 3D and Fig. S8A in Supporting information) and M2-like TAM (Fig. 3E and Fig. S8B in Supporting information) decreased and the M1-like TAM population increased (Fig. 3F and Fig. S8C in Supporting information). Moreover, the M1/M2 ratio of the drug treatment groups was significantly improved (Control:0.61; P-ip&L-po:1.28; P&L@Gel:1.97) (Fig. 3G). Also, as shown in Figs. 3H, I and Fig. S8D (Supporting information), compared with normal saline, P&L@Gel and P-ip&L-po could increase the levels of CD4+ T cells by approximately 9% and 7% as well as infiltrated CD8+ T cells by approximately 14% and 2%, which could alleviate the dilemma that poor T cells existed inside the tumor microenvironment and enhance the therapy effects of immune checkpoint blockade [2]. In addition, the infiltration of Tregs in the tumor microenvironment was further investigated. The level of Tregs was found lower in drug treated groups (Control: 30.67%; P-ip&L-po: 22.72%; P&L@Gel: 20.61%), and no significant difference was detected between the P&L@Gel group and the P-ip&L-po group (Fig. 3J and Fig. S8E in Supporting information). Taken together, compared with saline-treated group, mice in P-ip&L-po and P&L@Gel groups showed improved TME and enhanced immune effects.

Compared with P-ip&L-po, P&L@Gel raised the level of T cells especially CD8+ T cells from 9.75% to 21.06% (Fig. 3I and Fig. S8D in Supporting information) as well as the ratio of M1/M2 from 1.28 to 1.97 (Fig. 3G) and decreased the infiltration of TAMs by 17.73% (Fig. 3D and Fig. S8A), indicating that the immune effects were activated more thoroughly by P&L@Gel. These results were due to high accumulation of drugs in tumor site after topical use of P&L@Gel (Fig. 1E), and also might related to that P&L@Gel could prolong the normalization window of the tumors. More research had verified that excessive pruning of tumor vessels would aggravate tumor hypoxia and shorten the normalization window, which was not conducive to the formation of tumor immune microenvironment [30,31]. It was important to choose an appropriate biomarker to judge whether the dose of antiangiogenic promoted vascular normalization or led to excessive pruning of tumor vessels. As reported [30], the increase of tumor-infiltrating CD8+ T cells, which had strong correlation with vascular normalization, could be a potential biomarker to choose the optimal drug dose. In this study, although the local concentration of drugs was much higher in P&L@Gel group, a significant increase in the level of CD8+ T cells detected (Fig. 3I) verified that the dose of LEN could promote the vascular normalization without causing tumor vessels excessive pruning. However, in the P-ip&L-po treated group, the degree of vascular normalization was weaker due to the low accumulation of LEN in tumor sites. Moreover, the high concentration of anti-PD1 in tumor site after P&L@Gel treatment could also induce the normalization of tumor vessels by CD4+ T cells and CD8+ T cells through IFN-γ pathway [14]. To sum up, the strongest immunity could be activated in P&L@Gel treated group owing to the prolonged window of vascular normalization carried by LEN and anti-PD1.

The changes of body weight, blood routine indexes, blood biochemical indexes, secretion of inflammatory factor and histological section were measured to detect the safety of P&L@Gel. No mice died by treatment and no severe body weight loss was observed in all groups during the whole treatment (Figs. 2B and D), indicating that all formulations had little effect on mice survival. Due to the rapid growth of tumors, mice in the control group and the blank gel group gained faster weight than mice in the other groups.

The important hematological indicators including HGB, WBC, RBC, PLT and GR were analyzed firstly in mice of all groups. The mice in control group and blank gel group were executed on the 10^{th} day, so their hematological indicators on the 17^{th} day were lost (Fig. 4A and Figs. S9A-C in Supporting information). As shown in Figs. S9A and B, on day 0 and the 17^{th} day, no significant changes in HGB and RBC were observed in these mice of subcutaneous ectopic tumor model. However, the level of WBC on the 17^{th} day was higher than that on day 0 in all groups (Fig. S9C), which may be due to tumor-associated inflammation occurred with the development of cancer [32]. Moreover, the level of PLT in the blood of mice treated with P-ip&L-po increased significantly on the 17^{th} day (Fig. 4A) while there was no significant change in other groups. The high level of PLT would increase the risk of vascular embolism [8]. Similar results were obtained on the mice of incompletely resected CT26-tumor model (Figs. S9F-I in Supporting information), the PLT level in P-ip&L-po group was significantly higher than other two groups (Fig. S9G). Besides, the GR level of mice treated with P-ip&L-po decreased on the 22^{nd} day (Fig. S9J in Supporting information), which may lead to infection and was consistent with reports that LEN might reduce the count of GR in the blood revealed from the data of clinical trials [33].

In order to monitor the hepatic function and renal function of mice after long-term treatment, the main biochemical parameters, including ALT and AST (Fig. 4B and Fig. S9D in Supporting information, both were functional parameters of the liver) as well as UA and CREA (Fig. 4C and Fig. S9E in Supporting information, both were functional parameters of the kidney) were analyzed. As shown in Fig. 4B and Fig. S9D, no significant difference among all groups on the level of AST was observed, while the ALT level of mice in P-ip&L-po group was obvious higher than that in other groups. Besides, the concentration of CREA in serum remained at the same level in all groups (Fig. S9E), while more UA secreted in serum was detected in the P-ip&L-po group (Fig. 4C). These results were related to the different profiles of LEN biodistribution in the P-ip&L-po and P&L@Gel groups. As shown in Fig. 1E, in the P-ip&L-po group, majority of the drugs were accumulated in serum (9.61%), liver (50.09%) and kidney (31.20%) and distributed less to the tumor site (<2%), which may lead to weaker anti-tumor efficacy and stronger side effects. However, in the P&L@Gel group, the majority of LEN (~87%) was highly accumulated in the tumor site and rarely distributed in liver (10%) and kidney (0.79%). Next, hematoxylin & eosin (H&E) staining was performed to verify whether the organic injury had been caused. As presented in Fig. S9K (Supporting information), negligible histological damage or inflammation lesions were detected in the main organs of mice in all groups, illustrating that almost no organic injury was occurred. Taken together, these two risen parameters indicated that the mice in P-ip&L-po group may had some liver and kidney damage, while these indicators in P&L@Gel did not change significantly compared with saline-treated group, further demonstrating the superiority of hydrogel.

According to the clinical trials, PPES is one of the most common any-grade adverse events (AEs) after oral administration of LEN [34]. It often occurs on the palms and soles, and starts with erythema and edema, and then proceeds to severe edema, blisters [35]. In order to detect whether the topical delivery of P&L@Gel could relieve this side effect, the inflammatory cytokines in paws, including Interleukin-1α (IL-1α), Interleukin-1β (IL-1β) and Interleukin-6 (IL-6), were detected by ELISA [36,37]. As shown in Figs. 4D-F, the secretion of IL-1α and IL-1β were markedly increased in P-ip&L-po treated group. And the average secretion of IL-6 in this group was higher than others. However, this indicator in P&L@Gel treated group showed no significant changes compared with control group. From the H&E staining images, no significant pathology changes of the skin were found between the P-ip&L-po treated group and other groups (Fig. S10 in Supporting information), indicating that the side effect caused by LEN was relatively mild. To sum up, these results demo nstrated that PPES may have occurred in the mice received oral administration of LEN, while the topical hydrogel could successfully relieve or avoid PPES.

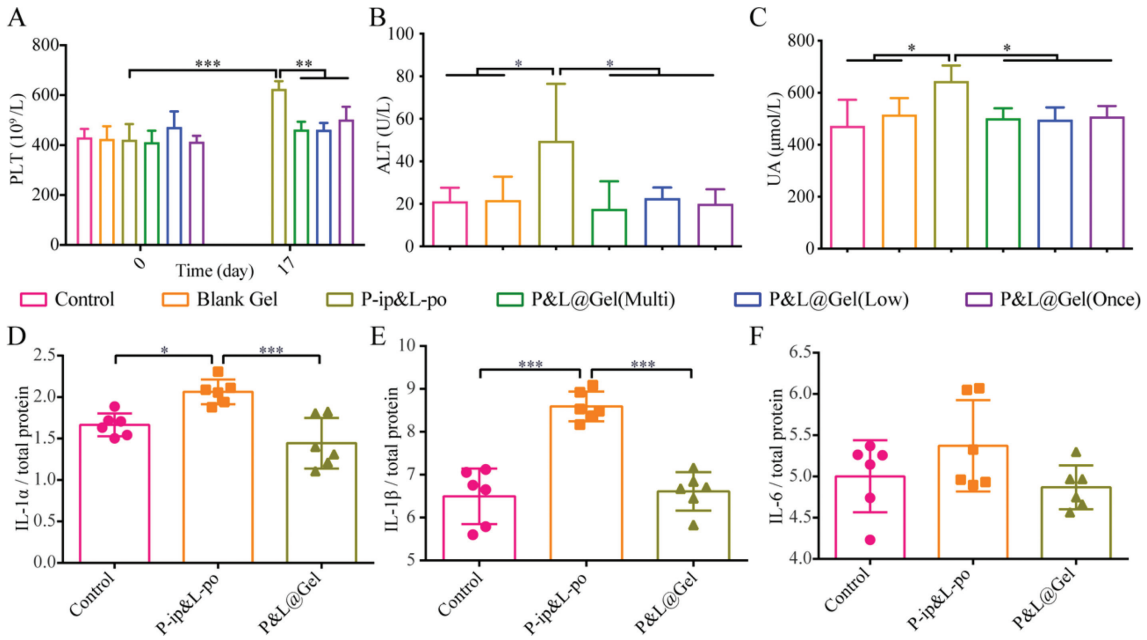

Fig. 4. *In vivo* safety evaluation of P&L@Gel. (A) The levels of PLT in the serum of mice on day 0 and the 17th day ($n = 5$). The levels of ALT (B) and UA (C) in the serum of mice on the 17th day ($n = 5$). The levels of IL-1α (D), IL-1β (E) and IL-6 (F) secreted inside the paw tissues ($n = 6$). Data was presented as mean ± S.D. $^{*}P < 0.05$, $^{**}P < 0.01$, $^{***}P < 0.001$.

In addition, PLGA-PEG-PLGA (ReGel®) has been approved for clinical application due to its convenient one-pot synthesis and good safety profiles [17,18]. Among these preparations, it was worth noting that a formulation of paclitaxel based on ReGel® named OncoGel™, was enrolled in cilinial trials, designed for local delivery of paclitaxel to solid tumors to provide targeted cytotoxicity without the systemic toxicities [17]. It could be foreseen that the application of ReGel® as a topical treatment gel material had promising clinical application. Furthermore, since the surgical wound in mice was relatively small, the gel preparation was injected into the tumor resection cavity in this study. Spray can be applied to evenly administer drugs to the wound for large animals in the future, which can further broaden the application of this formulation in clinic.

In this study, the *in-situ* thermosensitive PLGA-PEG-PLGA hydrogel containing anti-PD1 and LEN has been successful developed for tumor therapy. The P&L@Gel could exhibit a higher tumor accumulation of two drugs, and show much better anti-tumor immunotherapy effect than P-ip&L-po. On CT26 tumor model, same tumor-inhibiting effects could be obtained by peritumoral administration of P&L@Gel with one-eighth dose of P-ip&L-po. More importantly, P&L@Gel could significantly enhance local T cell infiltration and cytokine secretion such as IFN-γ and TNF-α, decrease Treg infiltration, reprogram the TAM phenotype, and thus notably improve immune response in mice. In addition, local administration of P&L@Gel showed a higher safety than P-ip&L-po. Overall, the injectable *in-situ* hydrogel containing angiogenesis inhibitor and immune checkpoint blockage provides a promising platform for tumor therapy.

Declaration of competing interest

The authors declare that they have no known competing financial interests or personal relationships that could have appeared to influence the work reported in this paper.

Acknowledgments

This work was supported by National Natural Science Foundation of China (Nos. 81690264 and 81973259) and the Open Project from Key Laboratory of Carcinogenesis and Translational Research, Ministry of Education/Beijing.

Supplementary materials

Supplementary material associated with this article can be found, in the online version, at doi:10.1016/j.cclet.2022.108104.

References

[1] P. Sharma, J.P. Allison, Science 348 (2015) 56–61.
[2] T. Tang, X. Huang, G. Zhang, et al., Signal Transduct. Target. Ther. 6 (2021) 72.
[3] Y. Hu, L. Lin, Z. Guo, et al., Chin. Chem. Lett. 32 (2021) 1770–1774.
[4] A.I. Matos, B. Carreira, C. Peres, et al., J. Control. Release 307 (2019) 108–138.
[5] W.S. Lee, H. Yang, H.J. Chon, et al., Exp. Mol. Med. 52 (2020) 1475–1485.
[6] K. Furukawa, T. Nagano, M. Tachihara, et al., Molecules 25 (2020) 3900.
[7] M. Yi, D. Jiao, S. Qin, et al., Mol. Cancer 18 (2019) 60.
[8] Z.T. Al-Salama, Y.Y. Syed, L.J. Scott, Drugs 79 (2019) 665–674.
[9] Y. Wang, M. Jiang, J. Zhu, et al., Biomed. Pharmacother. 132 (2020) 110797.
[10] A.X. Zhu, R.S. Finn, M. Ikeda, et al., J. Clin. Oncol. 38 (2020) 4519.
[11] T.F. Greten, C.W. Lai, G. Li, et al., Gastroenterology 156 (2019) 510–524.
[12] L. Torrens, C. Montironi, M. Puigvehí, et al., Hepatology 74 (2021) 2652–2669.
[13] S. Arora, S. Balasubramaniam, W. Zhang, et al., Clin. Cancer Res. 26 (2020) 5062–5067.
[14] K. Shigeta, M. Datta, T. Hato, et al., Hepatology 71 (2020) 1247–1261.
[15] Y. Kato, K. Tabata, T. Kimura, et al., PLoS One 14 (2019) e0212513.
[16] D.C. Mo, P.H. Luo, S.X. Huang, et al., Int. Immunopharmacol. 91 (2021) 107281.
[17] N.L. Elstad, K.D. Fowers, Adv. Drug Deliv. Rev. 61 (2009) 785–794.
[18] G.M. Zentner, R. Rathi, C. Shih, et al., J. Control. Release 72 (2001) 203–215.
[19] X. Zhou, X. He, K. Shi, et al., Adv. Sci. 7 (2020) 2001442.
[20] H.F. Darge, A.T. Andrgie, E.Y. Hanurry, et al., Int. J. Pharm. 572 (2019) 118799.
[21] S. Cui, L. Yu, J. Ding, Macromolecules 51 (2018) 6405–6420.
[22] A. Alexander, J.Khan Ajazuddin, et al., J. Control. Release 172 (2013) 715–729.
[23] P. Wang, W. Chu, X. Zhuo, et al., J. Mater. Chem. B 5 (2017) 1551–1565.
[24] H. Ma, C. He, Y. Cheng, et al., Biomaterials 35 (2014) 8723–8734.
[25] L. Huang, Y. Li, Y. Du, et al., Nat. Commun. 10 (2019) 4871.
[26] Y. Yamamoto, J. Matsui, T. Matsushima, et al., Vasc. Cell 6 (2014) 18.
[27] O. Tohyama, J. Matsui, K. Kodama, et al., J. Thyroid Res. 2014 (2014) 638747.
[28] L. Tian, A. Goldstein, H. Wang, et al., Nature 544 (2017) 250–254.
[29] J. Shen, Z. Xiao, Q. Zhao, et al., Cell Prolif. 51 (2018) e12441.
[30] Y. Huang, S. Goel, D.G. Duda, et al., Cancer Res. 73 (2013) 2943–2948.
[31] Y. Huang, J. Yuan, E. Righi, et al., Proc. Natl. Acad. Sci. U. S. A. 109 (2012) 17561–17566.
[32] S. Shalapour, M. Karin, Immunity 51 (2019) 15–26.
[33] T. Terashima, T. Yamashita, N. Takata, et al., Hepatol. Res. 51 (2021) 190–200.
[34] S. Takahashi, N. Kiyota, T. Yamazaki, et al., Future Oncol. 15 (2019) 717–726.
[35] S. Hiromoto, T. Kawashiri, N. Yamanaka, et al., Sci. Rep. 11 (2021) 8964.
[36] X. Hu, M. Dong, X. Liang, Z. Liu, Q. Li, Int. J. Nanomedicine 16 (2021) 471–480.
[37] N. Yokomichi, T. Nagasawa, A. Coler-Reilly, et al., Hum. Cell 26 (2013) 8–18.